

AIAA PAPER
75-163

MECHANISM OF IGNITION IN SHOCK WAVE INTERACTIONS
WITH REACTIVE LIQUID DROPLETS 11p

by
T. H. PIERCE, C. W. KAUFFMAN,
and
J. A. NICHOLLS
The University of Michigan
Ann Arbor, Michigan



**AIAA 13th Aerospace
Sciences Meeting**

PASADENA, CALIF. / JANUARY 20-22, 1975

For permission to copy or republish, contact the American Institute of Aeronautics and Astronautics,
1290 Avenue of the Americas, New York, N.Y. 10019.

M75-10502

AIAA PAPER 75-163

MECHANISM OF IGNITION IN SHOCK WAVE INTERACTIONS
WITH REACTIVE LIQUID DROPLETS*

T. H. Pierce,** C. W. Kauffman,† and J. A. Nicholls††
The University of Michigan
Department of Aerospace Engineering
Ann Arbor, Michigan 48105

Abstract

A detailed qualitative analysis of the processes leading to the explosive ignition of a reactive liquid droplet that is suspended in a gas-phase oxidizer and subjected to the passage of a shock wave, is presented. The interval of time between shock wave passage and ignition is described by identifying a two-stage process which consists of a period of relative reactive dormancy that is followed by a chemical induction period leading to the thermal explosion of reactant that has been stripped from the liquid drop, vaporized, and mixed with the gas-phase oxidizer. The results of first-order calculations based on this model are presented and compared with experimental data for diethylcyclohexane drops in oxygen.

Introduction

Detonations which occur in reactive media consisting initially of liquid fuel droplets suspended in a gas-phase oxidizer have been studied both theoretically¹ and experimentally^{2,3}. The most important features of these detonations are their extremely long reaction zones (which reduces their propagation velocity when they occur within ducts) and the appearance of numerous pressure spikes within the reaction zone (as much as 100% above the shock pressure.) These features are ultimately connected with the manner in which the liquid droplets are converted to the vapor phase, and to how the two vapor phase reactants then mix and ignite. The conversion process involved is that of the interaction of the detonation leading shock wave with each of the drops individually in the spray. Much empirical data have been gathered which have shown the major characteristics of this particular process for the case of shock interaction with non-reacting drops⁴⁻⁸. Unfortunately, much less information is available for the case of reacting drops, which forms the subject of interest here^{9-11,14}.

Both non-reacting and reacting drops share certain features of a shockwave interaction. While the shock wave is passing over the initially stationary droplet, very little of consequence occurs. In particular, the drop does not change its velocity during this period while the surrounding gas is accelerated. This produces a flow field around the droplet. If the shock strength is sufficient, the free stream velocity

can be supersonic with respect to the drop. Under these circumstances, a bow shock, wake shock, and other characteristics of supersonic flow over a sphere¹² are apparent (Fig. 1). The drop subsequently contracts along an axis which is parallel to the free stream, and expands in the transverse direction, so that the frontal area exposed to the flow increases with time. The drop also begins to accelerate in the direction of the moving shock.

The fluid near the surface in the drop is set in motion by the boundary layer gases of the convective flow. The liquid boundary layer separates from the droplet and is apparently broken up into a spray of droplets whose diameter is of the order of the boundary layer thickness. This "microspray" (μ spray) is thereby introduced into the near wake region of the parent droplet. It appears that, at the same time, a Taylor instability occurs on the front surface of the parent drop, producing waves whose amplitudes grow and will eventually cause "catastrophic" disintegration of the parent drop¹³.

After a certain period of time following passage of the incident shock ($t = t^*$), the parent drop ceases its transverse growth; the frontal diameter thereafter decreases. Whether or not catastrophic breakup due to Taylor instabilities has occurred by this point is not clear. Nonetheless, if the parent drop is reactive, it is somewhat after this time that the ignition of evaporated μ spray occurs in the near wake region. The ignition is explosive in character, producing a blast wave. The explosive ignition accounts for the reaction zone pressure spikes in a two-phase spray detonation.

Beyond this ignition, the process of mass stripping from the parent drop (or its fragments in the event of catastrophic breakup) continues until nothing remains of it. If ignition has occurred, in the reactive case, the continued stripping supplies fresh fuel to the wake region where it is then consumed. This post-ignition combustion process is usually relatively "smooth"; occasionally, however, multiple explosive ignitions occur in sequence.

Only incident shocks of sufficient strength produce explosive ignition. As a rule, $M_s > 3$

* Work supported by NASA Grant NGL 23-005-336 under the direction of R. J. Priem.

**Presently Assistant Professor, Department of Mechanical and Aerospace Engineering, North Carolina State University, Raleigh, North Carolina 27607. Member AIAA.

† Presently Associate Professor, Department of Aerospace Engineering, University of Cincinnati.

††Professor of Aerospace Engineering. Member AIAA.

is required, typically. In what follows, it will therefore be assumed that the incident shock is of this strength, and also that the resulting flow field around the parent droplet is initially supersonic.

The capacity to describe the sequence of events, which was qualitatively outlined above, in sufficient detail as to allow reasonable prediction of the time between incident shock contact with a reactive drop and its explosive wake ignition, is of obvious interest. Kauffman¹⁴ suggested a model in which groups of stripped μ spray, which move rearward into the wake region, remain as they move in volume elements of fixed identity and fixed geometry. The μ spray in each such volume element evaporates, and the vapor produced mixes homogeneously throughout the element. Ignition is identified with that element in which the concentration of fuel is largest; ignition times are assessed from the interval separating incident shock contact and the formation of this element.

Pierce¹⁵ treated a simple model in which stripped μ spray enters the wake and therein evaporates and reacts with the hot oxidizer. The energy thus liberated is conducted away to the external flow until the total evaporation rate (which controls the energy release rate) becomes so large that thermal energy begins to accumulate in the wake region. The point in time at which this occurs is prescribed to be the instant of ignition, since as the temperature of the region increases, the processes responsible for further energy liberation are accelerated.

Recently, Fishburn^{13,16} has suggested that the density of μ spray drops (in the wake region of the parent drop) during the first period following incident shock passage, produces local fuel vapor concentrations which are too low to support explosive ignition. That is, boundary layer stripping of the contiguous parent droplet is considered to be too slow a process to allow for high μ spray densities. Therefore it is argued that fragmentation of the parent drop, through Taylor instabilities, must first occur; each fragment then individually strips, resulting in a much higher rate of μ spray production. Again, the μ spray drops enter the wake, evaporate and react, and a chemical induction time is added (to the time until fragmentation occurs) to obtain the overall ignition delay.

Each of these theories shows some degree of agreement with the available experimental ignition time data^{9,11,14}, yet none, in itself, is able to convincingly explain all of the observations made of the ignition process. The ability to extend any one of these computations to reliably include a wide range of fuel/oxidizer combinations is rather questionable. It is the purpose of the present exploratory study to contribute towards the development of a unified theory of shock induced reactive droplet ignition.

Theoretical Model

In its present form the sequence of events leading to explosive ignition is considered as comprised of two separate intervals; namely, a

"dormant" period, followed by an "active" period. These could also be described as mechanical and chemical induction periods. As such, this model is similar in kind to Fishburn's two-stage model. That is, if the same terminology were applied to that model, the "dormant" and "active" periods would correspond to the intervals before and after parent drop fragmentation, respectively. It is to be emphasized at the outset that the two periods in the following formulation both differ qualitatively (as well as quantitatively) from the Fishburn model.

Dormant Period

This period begins upon initial contact by the incident shock with the spherical droplet in its undisturbed, motionless state. Four processes are initiated. First, the droplet begins to accelerate. This in turn initiates the development of Taylor instabilities on the forward surface. At the same time, the droplet begins to flatten, and the boundary layer formation in liquid surface commences.

Complete boundary layer formation requires a nontrivial induction time¹⁷. However, it is believed that the mass stripping process begins well before the liquid boundary layer is fully developed. This is based on the many early-time photographs such as in Fig. 2, as well as on mass loss measurements⁵. In any event, it is clear that the mass loss rate accelerates with increasing time during this period. In fact, Reinecke⁶ has obtained a reasonable empirical correlation for mass loss, assessed from x-ray photographs of stripping water drops, which is

$$\frac{m}{m_0} = \frac{1}{2} \left[1 + \cos \pi(t/t_s) \right] \quad (1)$$

The mass, m , of the droplet at any time, t , during the breakup process is thus correlated with its initial mass, m_0 , and the time to complete disintegration, t_s (stripping time).

As the droplet continues to flatten, its frontal diameter increases rapidly. Fluid in the liquid boundary layer, which travels from the forward stagnation point to the maximum perimeter before separating into μ spray travels progressively further before being stripped off. This, as well as the fact that the liquid boundary layer becomes more fully developed with passing time, leads to the expectation of increased μ spray size with increasing time.

No widely accepted means of computing μ spray sizes and separation velocities exists. There is some agreement, however, that the μ spray diameter should be of the order of the liquid boundary layer thickness just prior to its separation^{14,15}. Most analytical estimates predict μ spray diameters of the order of 1% of the parent drop diameter, which roughly agrees with what experimental evidence is available^{4,7}.

For example, the separation process can be envisioned to proceed in two stages: First, an annular sheet or film of fluid is shed from the drop periphery, and second, this sheet breaks

up into the μ spray drops by means of a process similar to that which occurs in the breakup of a free liquid jet¹⁸. The micromist drops can, by that analogy, be expected to have diameters which are approximately twice the thickness of the sheet. The sheet thickness itself is estimated by imposing conservation of mass and momentum on the fluid which enters it, between the positions just before separation (when the fluid is in the parent drop boundary layer) and just after separation (when the fluid is in the annular sheet and has a flat velocity profile.)

When the liquid boundary layer is assumed to have a Taylor velocity profile⁵, this particular means of analysis produces reasonable early-time mass loss rates and μ spray sizes¹⁵. In addition, the velocity of the μ spray when it separates from the parent drop, u_d , can be readily derived to the form

$$\frac{u_d}{u_c} = \frac{A}{\sqrt{2}}, \quad (2)$$

in which u_c is the relative convective flow velocity, while

$$A = \left(\frac{\rho_2 \mu_2}{\rho_L \mu_L} \right)^{1/3} \quad (3)$$

and $\rho_2, \mu_2, \rho_L, \mu_L$ are the densities and viscosities of the liquid and of the free stream convective flow.

It is reasonably clear that boundary layer stripping cannot account for the mass loss rates over the entire breakup time. The surface wave concept of Collins¹⁹ or the Taylor instability theory of Fishburn¹³ is needed at later times to explain the high stripping rates. It is believed, however, that simple boundary layer stripping predominates the early stages of breakup, and Eq. (2), in spite of its crudeness, serves to show that $u_d/u_c = O(10^{-1})$ for typical intermediate shock strengths and typical fuel/oxidizer combinations. That is, the fluid separates from the parent drop at velocities which are considerably lower than the prevailing free stream gas velocity.

The velocity with which the point of separation moves in the transverse (or, radial) direction due to drop flattening may be evaluated from the well accepted empirical form²⁰

$$\bar{D} = 1 + \alpha \bar{T} \quad (4)$$

in which \bar{D} is the ratio of parent drop frontal diameter at time t to its initial/undisturbed diameter, D_0 , and

$$\bar{T} = \frac{u_2}{D_0} \beta^{1/2} t \quad (5)$$

is the non-dimensional time, $\beta \equiv \rho_2/\rho_L u_2$, free stream gas velocity relative to the drop at $t = 0$, and α is a correlating coefficient whose value is $\alpha \approx 1.70$. From Eq. (4), the radial velocity, u_r , of the separation point is

$$u_r/u_c = (1/2) \alpha \beta^{1/2} (u_2/u_c). \quad (6)$$

The radial velocities computed from Eq. (6) show that u_r/u_c is also $O(10^{-1})$.

The inference from these two simple results is that in general the separated liquid film can be expected to turn in the direction of the prevailing local flow field while it is still contiguous with the parent drop (i.e. before breaking up into μ spray drops). When the external flow field is subsonic, the μ spray is in this fashion carried rearward, more or less parallel to the axis of symmetry. It is gradually accelerated, and ultimately reaches the convective flow velocity. An example of this is shown in Fig. 3.

When the flow field is supersonic, which is the case of interest here, it appears that the separated film is turned inward by the flow structure, in such a way that the μ spray is initially carried into the free shear layer of the near wake, above the recirculation zone. It subsequently becomes engulfed in the expanding recirculation zone itself, and most does not escape, having entered at low velocity. This results in a remarkably well-defined recirculation zone, as in Figs. 4 and 5.

In fact, the rearward velocity of the recirculation zone tip can be estimated by noting that its geometry remains roughly constant while the parent drop is growing. Since the droplet growth rate is given by Eq. (6), the rate of growth in recirculation zone length is simply

$$dL/dt = u_r \cot \beta \quad (7)$$

in which β is the recirculation zone angle with respect to the axis. For typical supersonic wakes, $4 < \cot \beta < 6$. Equation (7) then shows that $dL/dt \ll u_2$, even for the larger value of $\cot \beta$. The actual velocity of the recirculation zone tip, measured from streak photographs such as Fig. 4(b), agrees with the order of magnitude predicted by Eq. (7). (It should be observed that the recirculation zone is not filled by microspray in the subsonic case and so it is not visible on photographs such as Fig. 3.)

Within the recirculation zone, the trapped μ spray move with the low velocity vortices and evaporate. If a given μ spray drop is formed at time τ (measured after incident shock contact with the parent drop), with initial diameter $d_{M_0}(\tau)$, then its diameter at time t (i.e. after an interval $t-\tau$) can be approximated by the quiescent evaporation rate expression²¹

$$d_M(t, \tau) = \begin{cases} \left[d_{M_0}^2(\tau) - 2C(t - \tau) \right]^{1/2}, & t \leq t_{ex} \\ 0, & t \geq t_{ex} \end{cases} \quad (8)$$

in which

$$C = \frac{4k}{C_p \rho_L} \ln \left[1 + \frac{C_p}{\alpha} (T_g - T_L) \right], \quad (9)$$

where k is the coefficient of thermal

conductivity of the gas, T_g is the gas temperature and C_p its specific heat, and \mathcal{L} and T_L are the latent heat and temperature of the liquid μ spray drop. The time to extinction of the μ spray drop (complete evaporation), t_{ex} , is

$$t_{ex} - \tau = \frac{d_{M_0}^2(\tau)}{2C} \quad (10)$$

The rate of mass evaporation from this μ spray drop at time t is

$$\dot{m}_{ev}(t, \tau) = C_2 d_M(t, \tau), \quad (11)$$

where $C_2 = \pi \rho_L C/2$.

These formulae allow computation of the total amount of fuel vapor which has evaporated from all μ spray drops in the recirculation zone up to time t , taking into account the time varying initial μ spray size, in the following manner. First, the number of μ spray drops, δn , which are formed during an interval, $\delta \tau$, about time τ , is

$$\delta n(\tau) = \frac{\dot{m}(\tau) \delta \tau}{m_{M_0}(\tau)} \quad (12)$$

where $\dot{m}(\tau)$ is the parent drop stripping rate, at $t = \tau$, and $m_{M_0}(\tau)$ is the mass of the μ spray drops formed at that time; i.e. $m_{M_0}(\tau) = \rho_L \pi d_{M_0}^3(\tau)/6$. The contribution at time $t > \tau$ to the total μ spray evaporation rate from μ spray drops formed at $t = \tau$ is

$$\delta \dot{m}_{ev}(t) = \dot{m}_{ev}(t, \tau) \delta n(\tau)$$

or, in the limit,

$$d\dot{m}_{ev}(t) = C_2 d_M(t, \tau) \frac{\dot{m}(\tau)}{m_{M_0}(\tau)} d\tau. \quad (13)$$

Therefore, the total evaporation rate, at time t , due to all μ spray drops present in the recirculation zone at that time, is found by integrating Eq. (13) over all $\tau \leq t$; namely,

$$\dot{m}_{ev}(t) = C_2 \int_{\tau=0}^t \frac{\dot{m}(\tau) d_M(t, \tau)}{m_{M_0}(\tau)} d\tau, \quad (14)$$

and the total mass of fuel vapor evaporated from all μ spray drops prior to time t is

$$m_{ev}(t) = C_2 \int_{\hat{t}=0}^t \int_{\tau=0}^{\hat{t}} \frac{\dot{m}(\tau) d_M(\hat{t}, \tau)}{m_{M_0}(\tau)} d\tau d\hat{t}. \quad (15)$$

A simple parent drop stripping rate which can be used is

$$\dot{m}(\tau) = \frac{\pi m_0}{2t_s} \sin \frac{\pi \tau}{t_s}, \quad (16)$$

which derives from Eq. (1), by differentiation,

and the time varying μ spray size, $d_{M_0}(\tau)$ is obtained in the fashion described earlier. Then, upon appropriate selection of values for the parameters which appear in Eq. (9), the vapor accumulation in the recirculation zone, m_{ev} , can be computed from Eq. (15) as a function of time.

It is noted parenthetically that m_{M_0} is, of course, never actually zero, but that, on the other hand, $\dot{m}(\tau)$ is zero at $\tau = 0$. That is, actual parent drop stripping can begin only when the liquid boundary layer has developed to the point that its kinetic energy cannot be dissipated by the liquid surface, (i.e., by means of surface tension) at the point of separation. This occurs, approximately, when the balance

$$2\sigma_L \pi D = (1/2) \rho_L \pi D \int_0^{d_s} u_L^2(y, t) dy \quad (17)$$

occurs, in which σ_L is the liquid surface tension, $u_L(y, t)$ is the time-varying liquid boundary layer velocity profile (measured inward from the surface at the point of separation), D is the parent drop frontal diameter, and d_s is the thickness of the annular sheet, when it is separated. This concept of a "boundary layer induction time" is indeed similar in spirit to that of Ranger⁵, but it does not require that the boundary layer be fully established before initiation of stripping. For the present purposes, an estimate of the minimum film thickness from Eq. (17), was used to compute $m_{M_0}(0)$ required in Eq. (15).

Characteristic calculations from Eq. (15) are summarized in Figs. 6 and 7, for the case of diethylcyclohexane (DECH) drops in oxygen. The vapor accumulation, at the moment, t^* , of maximum droplet expansion, is shown in Fig. 6 as a fraction of the total mass removed from the parent drop up to that time, m_{st} . Figure 7 shows the maximum μ spray initial diameter, $d_{M_0}(t^*)$. That is, the initial diameter of the μ spray that enters the recirculation zone increases from $d_M(0)$ (an extremely small size) to $d_{M_0}(t^*)$ as t increases from $t = 0$ to $t = t^*$. The effect of initial pressure, P_1 , as well as parent drop initial diameter, D_0 , and incident shock Mach number, M_s is demonstrated. The extent of the evaporation which has occurred by t^* is surprisingly small for D_0 somewhat larger than 300μ .

The equivalence ratio*, ϕ , corresponding to the accumulation of fuel vapor within the recirculation zone at t^* , is shown on Fig. 8. It is observed that at reduced pressures and for small parent drop sizes, the equivalence ratio could reach significant values. The calculations indicate, however, that the accumulation rates are slow; i.e. $\dot{m}_{ev}(t)$ from Eq. (14) is never very large for parent drops which are larger than 300μ diameter.

*Equivalence ratio is defined as the quotient of actual fuel/oxidizer ratio to the stoichiometric fuel/oxidizer ratio, so that $\phi = 1$ represents the stoichiometric condition.

From these results, three conclusions can be drawn. First, the recirculation zone does not impulsively reach an extremely fuel rich condition (as was initially suspected). On the contrary, the region is generally quite lean. Second, in those cases for which m_{pv} is non-negligible, continuous reaction with the hot oxidizer will preclude accumulation of fuel vapor to the extent indicated in Fig. 8. Moreover, at time t^* , most of the liquid fuel which was stripped from the parent drop resides in its recirculation zone in the form of unevaporated μ spray. Therefore, there is little possibility that the recirculation zone can itself support an explosive ignition. In fact, when ignition occurs, the entire wake region is consumed except for the recirculation zone, as can be seen in Fig. 9.

Active Period

The frontal diameter of the parent drop reaches its maximum when $t = t^*$; t^* correlates roughly with $\bar{T} = 1.3$. Catastrophic breakup, as predicted by Fishburn¹³, would have occurred prior to this time; viz., approximately $\bar{T} = 0.9$. It is not completely clear as to whether or not this is in fact the case, and, in any event, the aggregate representing the remaining parent drop shows no abrupt change in velocity during this period. If it has been shattered into fragments, these fragments, as a closely packed group, evidently (thereafter) behave as a single (porous) body. Fragmentation would, of course, explain the accelerated stripping rates (which occur at about this time), but Collins' surface wave theory¹⁹ does so equally well. The experimental data available at this writing simply do not allow for discrimination between these two possibilities.

Nevertheless, it is not essential to the present phenomenological description of ignition that the cause for accelerated mass removal be actually identified, because a change in the stripping mechanism does not appear to be the single event that is primarily responsible for eventual explosive ignition. Instead, it appears that the termination of parent drop flattening, which allows the escape of substantial quantities of μ spray from the near wake region, is responsible for the final events leading to ignition. That is, μ spray which is shed during the period following time t^* is not engulfed by an expanding recirculation zone, but rather is injected outside of a shrinking near wake so that it becomes exposed to the high speed convective flow.

As the escaping μ spray begins to move rearward, it is itself accelerated, and this requires a small, but finite, amount of time. With a drag coefficient of unity, the equation of motion for a μ spray drop is simply

$$\frac{du_c}{dt} = -\frac{3}{4} \frac{\rho_2}{\rho_1} \frac{u_c^2}{d_M} \quad (18)$$

in terms of the relative convective velocity, u_c . For the case of constant d_M , this integrates to

$$u_c = u_{c0} \left(1 + \frac{3}{4} \frac{\rho_2}{\rho_1} \frac{u_{c0}^2 t}{d_M} \right)^{-1} \quad (19)$$

where u_{c0} is the relative velocity at separation. Equation (19) provides an upper bound on acceleration times. For $u_{c0} = u_2$, the time for a 10μ DECH drop to reach $u_c/u_{c0} = 0.3$ is $0(1 \mu\text{sec})$ corresponding to $M_c = 4$, and $P_1 = 1$ atm oxygen; the time to reach $u_c/u_{c0} = 0.1$ is $0(5 \mu\text{sec})$. Acceleration times increase linearly with μ spray diameter.

The μ spray that escapes at $t > t^*$ can be observed on streak photographs such as Fig. 4(b). Although the acceleration time of an escaped μ spray drop is very short, it can be expected to have been largely converted to the vapor phase during that period. The 10μ DECH drop in the above example has a Weber number, $We = (\rho_2 u_c^2 d_M)/\sigma$, which is $0(10^3)$, and this is still^c far above the minimum Weber number that corresponds to the stripping mode, $We = 15$. If the stripping mechanisms are not essentially different than those for larger drops, the time for this 10μ drop to strip is $0(1 \mu\text{sec})$. This is the same time order as its acceleration period. The "second generation" μ spray produced during this stripping process, whose diameters should be $0(10^{-1}\mu)$, would vaporize in negligible time orders.

If the stripping mechanism is unacceptable for these small μ spray drop sizes, rapid conversion of the escaped μ spray to the vapor phase can also be expected simply by convection assisted evaporation during the acceleration period. When the relative convective velocity is appreciable, as in the case of escaped μ spray drops, the quiescent evaporation rate, given by Eq. (8), should be replaced with²²

$$\frac{d d_M}{dt} = -\frac{C}{d_M} (1 + Re^{1/2} Pr^{1/3}), \quad (20)$$

in which $Re = (\rho_2 u_c d_M)/\mu_2$, and $Pr = \nu_2 Cp/k$. The second term in brackets can account for a five-fold increase in evaporation rate under typical conditions, reducing the characteristic evaporation time of the 10μ diameter drop from $200 \mu\text{sec}$ to $40 \mu\text{sec}$. Hence, if evaporation alone must account for the conversion of the μ spray to vapor, an appreciable amount of this conversion can be shown to occur during the acceleration period.

It is most probable that both stripping and simple evaporation occur simultaneously. Neither appears to cause complete conversion of the escaped μ spray to vapor; that is, the μ spray remains visible on photographs. However, for modeling purposes, complete conversion will be assumed.

Under that assumption, the essential feature of the parent drop disintegration process, beginning at t^* , is characterized by the impulsive continual injection of relatively large quantities of reactive vapor into the outer near wake region of the parent drop. This is somewhat similar phenomenologically to forward stagnation point

mass addition as it might occur in supersonic flow about a solid sphere or cylinder²³. By that comparison, vapor concentrations can be expected to decrease with increasing axial and radial distance within the wake; the greater variation would be in the radial direction. In fact, the assumption of constant radial vapor distribution with increasing axial distance is not wholly unreasonable, over the first few diameters of length. On the other hand, an assumption of radial uniformity in the vapor concentration would appear to be a rather dangerous oversimplification.

Each local element of mixed fuel vapor and oxidizer may for modeling purposes be regarded as a homogeneous chemical system which, at the instant of initial mixing, has a specific mixture ratio and initial temperature. As reaction proceeds toward "equilibrium", the products remain within the element. Diffusion and thermal conduction between adjacent elements are ignored. The later was justified based on an estimate of laminar heat transfer over the time orders of interest. Each element therefore experiences an accelerated reaction rate due to self-heating. After a chemical induction time, τ_{chm} , the maximum rate of temperature rise is reached. The energy release rate at this time can be of explosive proportions; if so, it marks the point of wake ignition.

Now, the initial temperature in each element is a function of the vapor concentration there. That is, the maximum temperature of the fuel in the condensed phase is its boiling temperature at the prevailing local pressure. When the fuel changes phase and mixes with the oxidizer, the mixture temperature (assuming a mixing process which takes place at constant pressure) can be readily shown to be

$$T_i = \frac{T_b - \mathcal{L}/C_{pf}}{1 + \alpha} + \frac{\alpha T_2}{1 + \alpha}, \quad (21)$$

in which T_b is the boiling point of the liquid, T_2 is the static temperature of the oxidizer in the free stream prior to mixing, and

$$\alpha = \left(\frac{1 - \kappa_f}{\kappa_f} \right) \frac{C_{px}}{C_{pf}}. \quad (22)$$

Here, κ_f is the mass fraction of fuel vapor in the element, and C_{px} , C_{pf} are the constant pressure specific heats of the fuel vapor and oxidizer, respectively.

The self-heating process is initiated at this temperature. To assess the duration of the induction period, the Edelman-Fortune quasi-global reaction rate equation for hydrocarbon vapor combinations with oxygen²⁴ was used. This is

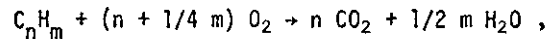
$$\frac{\partial C_f}{\partial t} \Big|_{chm} = -5.52 \times 10^8 p^{-.825} T C_f^{1/2} C_{O_2} \cdot \exp \left[(-1.22 \times 10^4)/T \right], \quad (23)$$

in which C_f and C_{O_2} are the fuel and oxidizer

concentrations in gram-moles/cm³, while the units of system pressure and temperature are atmospheres and Kelvin degrees.*

The induction period is assumed to proceed under a constant pressure condition. Thus, as heat is liberated by reaction, the element volume increases. Concentration changes are then due both to volumetric expansion and chemical reaction; the rate of energy liberation is determined from the latter. The fuel concentration in a constant pressure system can not be determined as a function of time from Eq. (23) alone. However, $T(t)$ may be obtained from this expression directly, because $\rho = \rho(T)$, where ρ is the total element mass density.

For any hydrocarbon, the stoichiometric equation is



and, temporarily assuming a fuel-lean system, the disappearance rate of oxygen molecules is assumed to be approximately governed by this equation. Hence,

$$\frac{\partial C_{O_2}}{\partial t} \Big|_{chm} = n_s \frac{\partial C_f}{\partial t} \Big|_{chm}, \quad (24)$$

in which $n_s = n + m/4$. Now for either species reactant, $C_i = \rho_i/w_i$, where ρ_i is its mass density and w_i its molecular weight. In terms of its mass fraction κ_i , this is $C_i = \kappa_i \rho/w_i$. Hence, Eq. (24) becomes

$$\frac{1}{w_{O_2}} \frac{\partial \kappa_{O_2}}{\partial t} \Big|_{chm} = \frac{n_s}{w_f} \frac{\partial \kappa_f}{\partial t} \Big|_{chm}, \quad (25)$$

and also Eq. (23) may be rewritten in the form

$$\frac{1}{w_f} \frac{\partial \kappa_f}{\partial t} \Big|_{chm} = -5.52 \times 10^8 p^{-.825} T^{1/2} \frac{\kappa_f^{1/2} \kappa_{O_2}}{w_f^{1/2} w_{O_2}} \cdot \exp \left[(-1.22 \times 10^4)/T \right]. \quad (26)$$

Of course, mass fractions are not affected by simple volumetric expansion, and so Eq. (25) can be integrated to give

*The use of Eq. (23) (by itself) to compute the rate of depletion of fuel provides a straightforward means for estimating approximate energy release rates. However, this empirical rate equation applies, strictly, only to the partial oxidation step in which the hydrocarbon reacts with diatomic oxygen to form diatomic hydrogen and carbon monoxide gases. It is not actually an overall global rate equation. It is important to emphasize this point because, used without its concomitant reaction steps (see Ref. 24), Eq. (23) predicts an improper dependence of the chemical induction time on the pressure of the system. However, the order of magnitude of the induction times are correctly predicted.

$$\kappa_{O_2} = \kappa_{O_2i} - \frac{n_s w_{O_2}}{w_f} (\kappa_{f_i} - \kappa_f) \quad (27)$$

Note that in Eq. (26), the units of ρ are gram/cm³.

Now, assuming a fuel lean condition, the heat of combustion per unit mass of fuel, \mathcal{H}_c , is approximately constant. Temperature increases due to combustion are then related to changes in quantity of fuel present through

$$d\kappa_f \Big|_{\text{chm}} = - \frac{C_p}{\mathcal{H}_c} dT \quad (28)$$

which is integrated to give

$$\kappa_f = \kappa_{f_i} - \frac{C_p}{\mathcal{H}_c} (T - T_i) \quad (29)$$

where C_p is the constant pressure specific heat of the mixture of gases in the element. Upon insertion of Eq. (29) in Eq. (27) we find

$$\kappa_{O_2} = \kappa_{O_2i} - \frac{n_s w_{O_2} C_p}{w_f \mathcal{H}_c} (T - T_i) \quad (30)$$

Then, combining Eq. (26) and Eq. (28-30) there obtains, after changing units, the equation for temperature rise in the element,

$$\frac{dT}{dt} = k_4 \frac{T^{1/2}}{p^{.325}} \kappa_{f_i}^{1/2} \kappa_{O_2i} \left[1 - \frac{C_p}{\kappa_{f_i} \mathcal{H}_c} (T - T_i) \right]^{1/2} \left[1 - \frac{n_s w_{O_2} C_p}{\kappa_{O_2i} w_f \mathcal{H}_c} (T - T_i) \right] e^{-2.2 \times 10^4/T} \quad (31)$$

which is in terms of the initial concentrations in the wake, κ_{f_i} and κ_{O_2i} . The constant k_4 has value

$$k_4 \equiv \frac{1.56 \times 10^{11}}{R^{1/2}} \left(\frac{w_f}{w_{O_2}} \right)^{1/2} \left(\frac{\mathcal{H}_c}{C_p} \right) \quad (32)$$

of which R is the specific gas constant of the mixture of gases in the element. Equation (31) is written with consistent English gravitational system units.

From Eq. (31), we find the time for the temperature in the element to reach any temperature T by integration, obtaining

$$\tau = \frac{p^{.325} E^{1/2} \psi(x_i)}{k_4 \kappa_{f_i}^{1/2} \kappa_{O_2i}} \quad (33)$$

where

$$\psi(x_i) \equiv \int_{x_i}^{\tilde{x}} \frac{e^{1/x} dx}{x^{1/2} \sqrt{1 - \theta_f(x-x_i)} [1 - \theta_{O_2}(x-x_i)]} \quad (34)$$

In this expression, $x \equiv T/E$, $E = 2.2 \times 10^4$ °R and

$$\theta_f = \frac{C_p E}{\kappa_{f_i} \mathcal{H}_c}$$

$$\theta_{O_2} = \frac{n_s w_{O_2} C_p E}{\kappa_{O_2i} w_f \mathcal{H}_c} \quad (35)$$

With T properly chosen, the value of τ computed from Eq. (33) may be regarded as characteristic of the induction time which precedes very rapid reaction. For example, T can be chosen as that temperature for which the integrand in Eq. (34) has its minimum. This would correspond to the moment of maximum rate of temperature rise, $(dT/dt)_{\text{max}}$.

Some simplification of Eq. (34) is possible by noting that $e^{1/x} / x^{1/2}$ decreases with extreme rapidity as x is increased. For typical values of θ_f , θ_{O_2} , and x_i , the integrand, therefore, becomes very small before $\theta_f(x - x_i)$ or $\theta_{O_2}(x - x_i)$ become significant compared to unity. It suffices, in general, to approximate Eq. (34) with

$$\psi(x_i) \equiv \int_{x_i}^{\tilde{x}} \frac{e^{1/x} dx}{x^{1/2}} \quad (36)$$

in which x can be chosen as virtually any value for which $e^{1/x} / x^{1/2} \ll e^{1/x_i} / x_i^{1/2}$. Equation (36) is then a universal function of x_i only, whose values appear on Fig. 10.

Each element of reactive gases in the near wake of the parent drop begins at a temperature T_i (or x_i) from Eq. (21), and has an induction time given by Eq. (33). It is clear from Fig. 10 that $\psi(x_i)$, and therefore τ , is extremely sensitive to T_i , and this in turn is mainly a function of initial mixture ratio. The mixture ratio is not only spatially variable within the wake, but its distribution is also not duplicated in practice between parent drops that are subjected to identical conditions, as is apparent from photographs such as Fig. 11. In spite of this, measured ignition times^{9,14} are reasonably reproducible

and so the sensitivity to the actual distribution of fuel vapor in the wake is apparently reduced by the mechanism of ignition that is involved.

An ignition mechanism which is consistent with these observations is as follows. It is postulated that "explosive ignition" of the entire near wake can be traced to homogeneous reaction which, occurring in a local reactive element, releases sufficient energy as to produce a shock wave capable of initiating detonation in the remainder of the wake. For the present purpose, a simplistic initiation requirement will be assigned; namely, that the local pressure rise due to homogeneous reaction must be equivalent to that across a Mach 3 shock wave.

The induction period of the homogeneous reaction is assumed to occur at constant pressure. However, once reaction rates become very large (i.e., $T \rightarrow \bar{T}$), the process is better approximated by a constant volume assumption. If most of the temperature rise occurs at these high reaction rates, the total local temperature rise is then simply

$$T_{\max} - T_i = \frac{\mathcal{H}_c \kappa_f}{C_v}, \quad (37)$$

which again assumes the fuel-lean condition, and C_v is the constant volume specific heat of the reactive element mixture. It is readily shown that if

$$\xi \equiv \frac{P_{\max}}{P_i} - 1,$$

the minimum mass fraction of fuel vapor required to produce a specified value of ξ is, from Eq. (37),

$$\kappa_f = \frac{T_i C_v \xi}{\mathcal{H}_c}. \quad (38)$$

For the equivalent pressure rise of a $M_s = 3$ shock, $\xi = 9$.

It is easily shown that the initial value of C_v in the element is related to κ_f through

$$C_v = \kappa_f C_{v_f} [1 + \alpha(\gamma_f/\gamma_x)], \quad (39)$$

where γ_f and γ_x are the ratios of specific heats of the fuel vapor and oxidizer, and α is defined by Eq. (22). Combining Eq. (38) with Eq. (39) and (21), and assuming $\gamma_f/\gamma_x = 1$ results in

$$\kappa_{f_{\min}} = 1/(1 + \omega), \quad (40)$$

where

$$\omega = \frac{C_{p_f}}{C_{p_x}} \frac{1}{T_2} \left(\frac{\mathcal{H}_c}{C_{v_f} \xi} + \frac{\mathcal{L}}{C_{p_f}} - T_b \right). \quad (41)$$

Elements with $\kappa_f < \kappa_{f_{\min}}$ do not possess sufficient energy to produce the pressure rise corresponding to ξ , while elements with $\kappa_f > \kappa_{f_{\min}}$ will require a longer induction time,

because of their reduced T_i . By taking $\mathcal{H}_c(\kappa_f)$ into account for fuel rich mixtures, a corresponding maximum κ_f can be found in similar fashion, but the fuel-lean element will always ignite first, due to its higher initial temperature. Hence $\kappa_{f_{\min}}$ in Eq. (40) is used to compute the minimum chemical induction time prior to wake detonation.

It is noted that the mass fraction of fuel vapor corresponding to the stoichiometric condition is easily found to be

$$\kappa_f^* = \frac{\lambda \phi_0^*}{1 + \lambda \phi_0^*}, \quad (42)$$

in which ϕ_0^* is the stoichiometric fuel-oxygen mass ratio, and λ is the initial mass fraction of oxygen in the oxidizer gas. (If the oxidizer is pure oxygen, $\lambda = 1$). If $\kappa_{f_{\min}} > \kappa_f^*$, explosive ignition is not possible; i.e., more energy is needed to initiate detonation than is available in any reactive element. Each element will proceed with local homogeneous reaction. This is also what should occur in elements having $\kappa_f < \kappa_{f_{\min}}$, which pass through $(dT/dt)_{\max}$ prior to τ_{\min} , and explains the appearance of luminous turbulent regions in the wake, which occur before explosive ignition is observed, cf. Fig. 9.

Results and Discussion

The time to explosive wake ignition, measured from first contact by the incident shock with the parent drop, is prescribed to be

$$t_{ig} = t^* + \tau_{chm} \quad (43)$$

in which t^* is the time for the parent drop to reach peak frontal diameter; namely,

$$t^* = (D_0 \bar{T}^*) / (u_2 \beta^{1/2}), \quad (44)$$

and τ_{chm} is obtained from Eq. (33) and (36) using $\kappa_{f_{\min}}$ from Eq. (42) to compute T_i in Eq. (21). The results from this computation are compared with experimental data on Fig. 12-14, which show the effects of Mach number, initial oxidizer pressure, and parent drop size.

The phenomenological description given here is not applicable to shock wave interactions with parent drops under conditions which would produce first generation spray whose characteristic quiescent evaporation times are significantly less than t^* . In such a case, explosive ignition within the recirculation zone, prior to t^* , is conceptually possible. Under typical conditions, this roughly restricts the present formulation to $D_0 > 100\mu$. It should also be pointed out that the chemical induction time is quite sensitive to the liquid boiling temperature, T_b , through its effect on T_i , while accurate high temperature boiling point data is not available for all hydrocarbons. The simplistic gas-phase detonation initiation criterion (the pressure rise due to local homogeneous reaction in the wake equals the equivalent of a $M_s = 3$ shock) could be replaced by a more realistic criterion.

However, the failure of the calculations to follow the trends in the experimental data (as pressure and Mach number are changed) derives primarily from the incorrect pressure dependence appearing in Eq. (33). This in turn is the result from having employed the quasi-global reaction rate equation, Eq. (23), as a global rate equation. Either the associated reaction steps must be included with Eq. (23), or a true global rate equation should be substituted for Eq. (23). The latter approach is to be preferred in the present application since it would lead to a closed-form expression similar to Eq. (33).

Figures

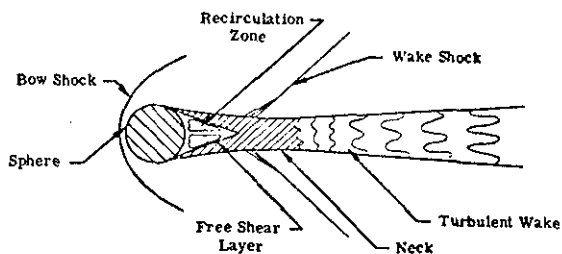


Figure 1. Supersonic Flow over a Sphere.

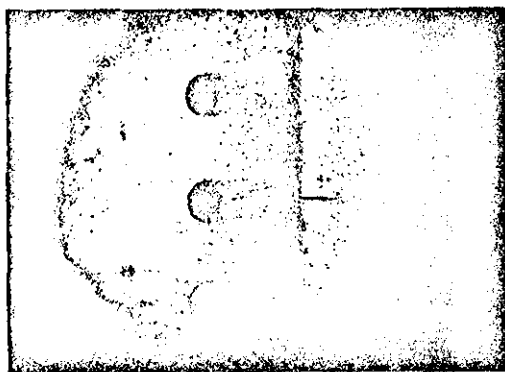
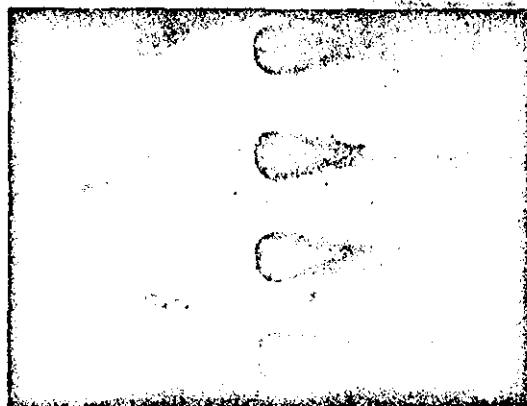


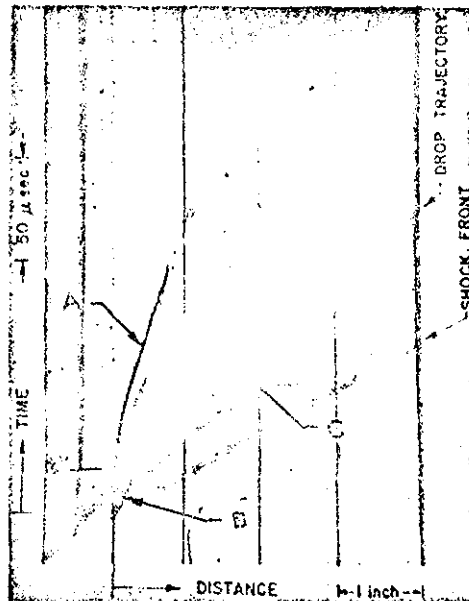
Figure 2. Shock Wave over a Water Drop, $d = 750 \mu\text{m}$, $M_S = 2.7$, $t = 2.6 \mu\text{s}$.



Figure 3. Shock Wave over a Water Drop, $d = 750 \mu\text{m}$, $M_S = 2.0$, $t = 15.8 \mu\text{s}$.



(a)



(b)

Figure 4. Shock Wave over a Water Drop; (A) Bow Shock, (B) Recirculation Zone (C) Escaped μspray (a) $d = 750 \mu\text{m}$, $M_S = 2.7$, $t = 4.4 \mu\text{s}$ (b) $d = 1400 \mu\text{m}$, $M_S = 3.34$.

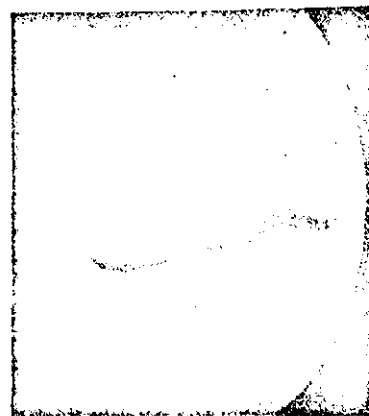


Figure 5. Shock Wave over a Water Drop, $d = 2700 \mu\text{m}$, $M_S = 3.5$, $t = 14 \mu\text{s}$.

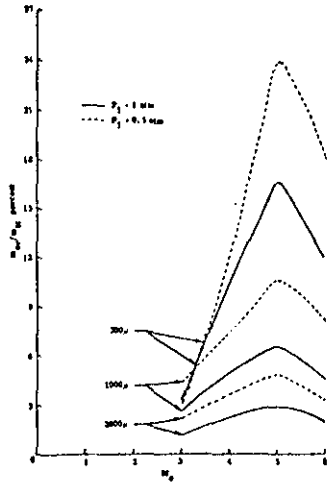


Figure 6. m_{ev}/m_{st} vs M_s .

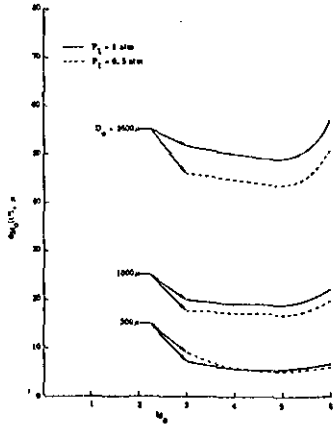


Figure 7. d_{M0} vs M_s .

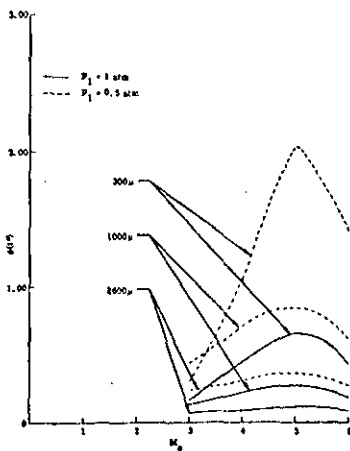


Figure 8. $\phi(t^*)$ vs M_s .

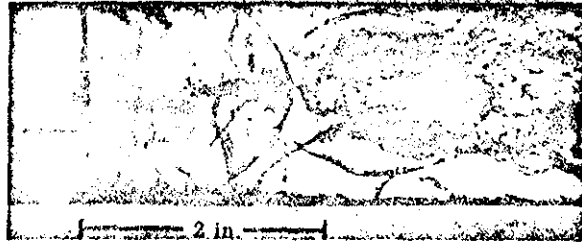


Figure 9. Detonation of Diethylcyclohexane Drops in Oxygen, $d = 2600 \mu$.

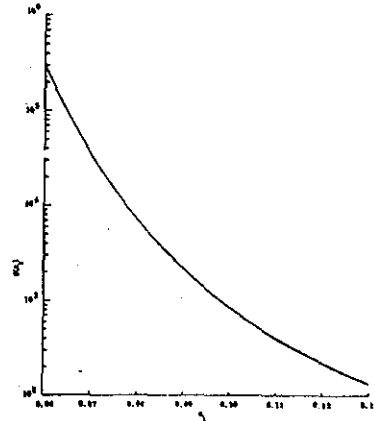


Figure 10. $\psi(x_j)$ vs x_j .

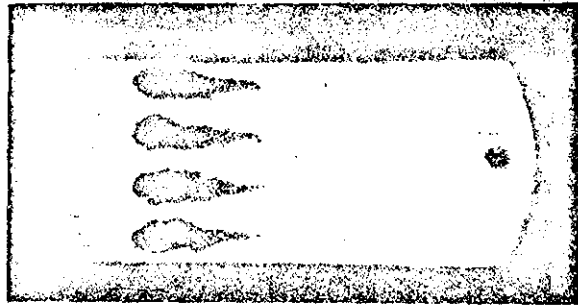


Figure 11. Shock Wave over Water Drops, $M_s = 3.25$, $t = 38.8 \mu s$.

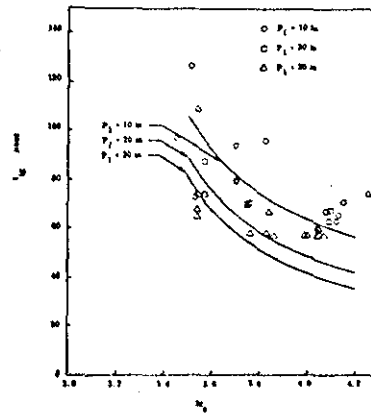


Figure 12. Ignition Time vs M_s , $d = 2130 \mu$.

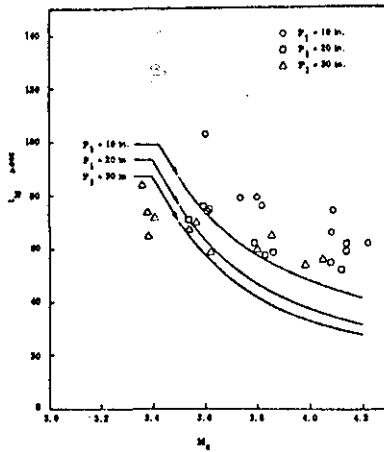


Figure 13. Ignition Time vs M_s , $d = 1520 \mu\text{m}$.

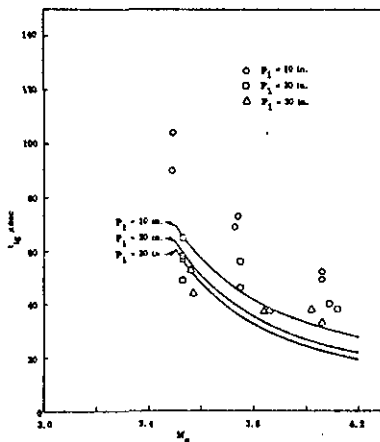


Figure 14. Ignition Time vs M_s , $d = 932 \mu\text{m}$.

References

1. Pierce, T. H., and Nicholls, J. A., "Time Variation in the Reaction-Zone Structure of Two-Phase Spray Detonations," Fourteenth Symposium (International) on Combustion, Pittsburgh, The Combustion Institute, 1973. pp. 1277 ff.
2. Pierce, T.H., and Nicholls, J.A., "Two-Phase Detonations with Bimodal Drop Distributions," *Astro. Acta.*, Vol. 17, 1972, pp. 703 ff.
3. Ragland, K.W., Dabora, E.K., and Nicholls, J.A. "Observed Structure of Spray Detonations," *Phys. Fluids*, Vol. 11, No. 11, 1968.
4. Ranger, A.A. and Nicholls, J.A., "Atomization of Liquid Droplets in a Convective Gas Stream," *Int. J. Heat Mass Transfer*, Vol. 15, 1972, p. 1203 ff.
5. Ranger, A.A. and Nicholls, J.A., "Aerodynamic Shattering of Liquid Drops," *AIAA J.*, Vol. 7, No. 2, February 1969.
6. Reinecke, W.G. and Waldman, G.D., "An Investigation of Water Drop Disintegration in the Region Behind Strong Shock Waves," Third International Conference on Rain Erosion and Related Phenomena, August 1970.

7. Aeschliman, D.P., "An Experimental Study of the Response of Water Droplets to Flows Behind Plane Shock Waves," Sandia Lab. Res. Report No. SC-RR-71 0540, 1971.
8. Reinecke, W.G. and McKay, W.L., "Experiments on Water Drop Breakup Behind Mach 3 to 12 Shocks," Sandia Lab. Res. Report No. SC-CR-70-6063, 1969.
9. Kauffman, C.W. and Nicholls, J.A., "Shock-Wave Ignition of Liquid Fuel Drops," *AIAA J.*, Vol. 9 No. 5, May 1971, pp. 880ff.
10. Lu, P.L. and Slagg, N., "Chemical Aspects of the Shock Initiation of Fuel Droplets," Picatinny Arsenal, AMCMS Code 552C.12.559, 1971.
11. Kauffman, C.W., Nicholls, J.A., and Olzmann, K.A., "The Interaction of an Incident Shock Wave with Liquid Fuel Drops," *Combustion Science and Technology*, Vol. 3, No. 4, 165 1971.
12. Berger, S.A., Laminar Wakes, Amer. Elsevier, New York, 1971.
13. Fishburn, B.D., "Boundary Layer Stripping of Liquid Drops Fragmented by Taylor Instability," Fourth International Colloquium on Gasdynamics of Explosions and Reactive Systems, 1973.
14. Kauffman, W.C., "Shock Wave Ignition of Liquid Fuel Drops," Ph.D. Thesis, Univ. of Michigan, 1971.
15. Pierce, T.H., "Experimental and Theoretical Study of the Structure of Two-Phase Detonation in Sprays," Ph.D. Thesis, Univ. of Michigan, 1972.
16. Fishburn, B.D., private communications, 1973.
17. Ranger, A.A., "Shock Wave Propagation Through a Two-Phase Medium," *Astronautica Acta*, Vol. 17, 1972, pp. 675 ff.
18. Dabora, E.K., "Production of Monodisperse Sprays," *Rev. Scientific Instruments*, Vol. 28, No. 4, 1967, pp. 502 ff.
19. Collins, R. and Charwat, A.F., "The Deformation and Mass Loss of Liquid Drops in a High-Speed Flow of Gas," *Israel J. of Technology*, Vol. 9, No. 5, 1971, pp. 453 ff.
20. Dabora, E.K., Ragland, K.W., and Nicholls, J.A. "Detonations in Two-Phase Media and Drop Shattering Studies," NASA CR-72421, May 1968.
21. Williams, F.A., "Progress in Spray-Combustion Analysis," Eighth Symposium (International) on Combustion, Williams and Wilkins Co., Baltimore, 1962.
22. Williams, F.A., Combustion Theory-The Fundamental Theory of Chemically Reacting Flow Systems, Addison-Wesley Publ. Co., Inc., 1965, p. 57.
23. Collins, D., Lees, L., and Roshko, A., "Near Wake of a Hypersonic Blunt Body with Mass Addition," *AIAA J.*, Vol. 8, No. 5, 1970.
24. Edelman, R.B., Fortune, O., and Weilerstein, G., "Some Observations on Flows Described by Coupled Mixing and Kinetics," Emissions from Continuous Combustion Systems, Plenum Press, N.Y., 1972.